Inorg. Chem. **2006**, *45*, 1888–1890

Inorganic Chemistry

Communication

Gold(I) η^2-Arene Complexes

Qing-Shan Li, Chong-Qing Wan, Ru-Yi Zou, Feng-Bo Xu,* Hai-Bin Song, Xiang-Jian Wan, and Zheng-Zhi Zhang*

State Key Laboratory of Elemento-Organic Chemistry, Nankai University, Tianjin 300071, China

Received October 27, 2005

The reaction of 9-{[*N*-*n*-propyl-*N*-(diphenylphosphino)amino]methyl}-anthracene (**1**) with Au(SMe_2)Cl yields complex **2** with an arm-opening configuration. The latter is treated with $AgClO_4$ to form complex **4** and then respectively reacted with acetonitrile, pyridine, and triphenylphosphine sulfide to afford novel gold(I) η^2-arene complexes **3a**–**c**, which have arm-closing configurations and feeble or weak fluorescence emissions. The observation can be attributed to charge transfer from the anthracene unit to the Au^+ ion. When the solution of **3a** or **4** in CH_2Cl_2 was added with 1 equiv of Ph_3P, complex **5** with the arm-opening configuration was formed and strong emission was restored.

As far as the group 11 metal−arene π complex is concerned, there are numerous η^2-bonding complexes between Ag^+ and the aromatic compound[1] and a few of the Cu^+ analogues;[2] surprisingly, no gold(1+) η^2-arene complex is reported. In 2003, we presented a new molecular design and gave the first gold(I) arene complex,[3] which is formed by the reaction of chelated diphosphine ligand 9,10-bis{[*N*-*n*-propyl-*N*-(diphenyphosphino)amino]methyl}anthracene with the Au^+ ion and adopts a η^6-coordination mode.

Herein we report some novel gold(I) η^2-arene complexes, their substitution reaction, and molecular responsive fluorescence spectral variation. In the first place, as shown in Scheme 1, 9-{[*N*-*n*-propyl-*N*-(diphenylphosphino)amino]-methyl}anthracene (**1**) was prepared by the reaction of 9-[(*N*-propylamino)methyl)]anthracene with Ph_2PCl. Then, the reaction of **1** with a stoichiometric amount of Au(SMe_2)Cl gave complex **2**, which converted to complexes **3a**−**c** by treatment with $AgClO_4$ and reaction with acetonitrile, pyridine, and triphenylphosphine sulfide, respectively.

Scheme 1

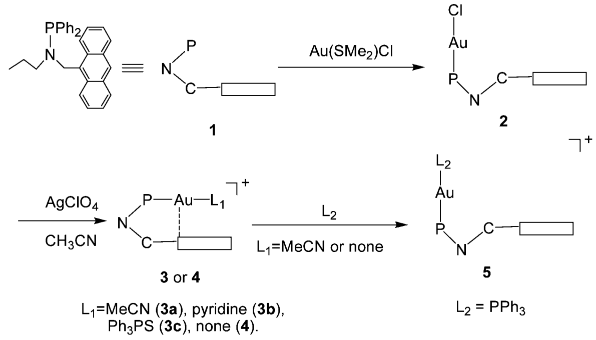

L_1=MeCN (**3a**), pyridine (**3b**), Ph_3PS (**3c**), none (**4**).

L_2 = PPh_3

The molecular structures of complexes **2** and **3a**−**c** have been determined by X-ray diffraction analysis.[4,5] As shown in Figure 1, the linear two-coordinated Au unit Cl(1)−Au(1)−P(1) (178.37°) is perpendicular to the anthracene ring in **2** (an arm-opening configuration). When the Cl atom is substituted by a CH_3CN, pyridine, or $Ph_3P{=}S$ molecule in elimination and coordination reactions, similar linear two-coordinated Au units P(1)−Au(1)−N(2) (179.59°; **3a**), P(1)−Au(1)−N(2) (177.07°; **3b**), and P(1)−Au(1)−S(1) (172.0°; **3c**) fold toward the anthracene planes (arm-closing configurations) (Figures 2 and 3 and the Supporting Information). The angles Au(1)−P(1)−N(1) are 111.06° (**3a**), 112.54° (**3b**),

---

* To whom correspondence should be addressed. E-mail: zzzhang@nankai.edu.cn (Z.-Z.Z.).

(1) (a) Munakata, M.; Wu, L. P.; Ning, G. L. *Coord. Chem. Rev.* **2000**, *198*, 171−203. (b) Lindeman, S. V.; Rathore, R.; Kochi, J. K. *Inorg. Chem.* **2000**, *39*, 5707−5716.

(2) (a) Turner, R. W.; Amma, E. L. *J. Am. Chem. Soc.* **1966**, *88*, 1877−1882. (b) Dines, M. B.; Bird, P. H. *J. Chem. Soc., Chem. Commun.* **1973**, 12. (c) Schmidbaur, H.; Bublak, W.; Huber, B.; Reber, G.; Muller, G. *Angew. Chem., Int. Ed.* **1986**, *25*, 1089−1090. (d) Conry, R. R.; Striejewske, W. S.; Tipton, A. A. *Inorg. Chem.* **1999**, *38*, 2833−2843.

(3) Xu, F. B.; Li, Q. S.; Wu, L. Z.; Leng, X. B.; Li, Z. C.; Zeng, X. S.; Chow, Y. L.; Zhang, Z. Z. *Organometallics* **2003**, *22*, 633−640.

(4) Crystal data for **2**: $C_{30}H_{28}AuClNP$, $M = 665.92$, monoclinic, space group $P2(1)/c$, $a = 9.595(3)$ Å, $b = 16.081(5)$ Å, $c = 17.189(5)$ Å, $\alpha = 90°$, $\beta = 92.575(5)°$, $\gamma = 90°$, $V = 2649.4(14)$ Å^3, $Z = 4$, $D_c = 1.669$ g cm^{-3}, $F(000) = 1304$, μ(Mo Kα) = 5.733 cm^{-1}, $T = 293(2)$ K, 5415 variables refined with 15 061 reflections with $I > 2\sigma(I)$ to $R = 0.0511$.

(5) Crystal data for **3a**: $C_{32}H_{31}AuClN_2O_4P$, $M = 770.97$, triclinic, space group $P1$, $a = 9.419(3)$ Å, $b = 12.900(4)$ Å, $c = 13.893(4)$ Å, $\alpha = 110.198(4)°$, $\beta = 104.902(5)°$, $\gamma = 95.536(4)°$, $V = 1498.8(7)$ Å^3, $Z = 2$, $D_c = 1.708$ g cm^{-3}, $F(000) = 760$, μ(Mo Kα) = 5.090 cm^{-1}, $T = 293(2)$ K, 6964 variables refined with 9710 reflections with $I > 2\sigma(I)$ to $R = 0.0415$. Crystal data for **3b**: $C_{35}H_{33}AuClN_2O_4P$, $M = 809.02$, orthorhombic, space group $Pna2(1)$, $a = 10.2098(10)$ Å, $b = 23.903(2)$ Å, $c = 13.1372(13)$ Å, $\alpha = 90°$, $\beta = 90°$, $\gamma = 90°$, $V = 3206.1(5)$ Å^3, $Z = 4$, $D_c = 1.676$ g cm^{-3}, $F(000) = 1600$, μ(Mo Kα) = 4.763 cm^{-1}, $T = 293(2)$ K, 7598 variables refined with 20 644 reflections with $I > 2\sigma(I)$ to $R = 0.0317$. Crystal data for **3c**: $C_{48}H_{43}AuClNO_4P_2S$, $M = 1024.25$, monoclinic, space group $P2(1)/c$, $a = 13.248(3)$ Å, $b = 16.329(3)$ Å, $c = 20.240(4)$ Å, $\alpha = 90°$, $\beta = 90.25(3)°$, $\gamma = 90°$, $V = 4378.7(15)$ Å^3, $Z = 4$, $D_c = 1.554$ g cm^{-3}, $F(000) = 2048$, μ(Mo Kα) = 3.586 cm^{-1}, $T = 293(2)$ K, 7652 variables refined with 20 309 reflections with $I > 2\sigma(I)$ to $R = 0.1154$. Diffractometer: Bruker Smart 1000 CCD diffractometer employing graphite-monochromatized Mo Kα radiation ($\lambda = 0.710\,73$ Å).

10.1021/ic051869r CCC: $33.50

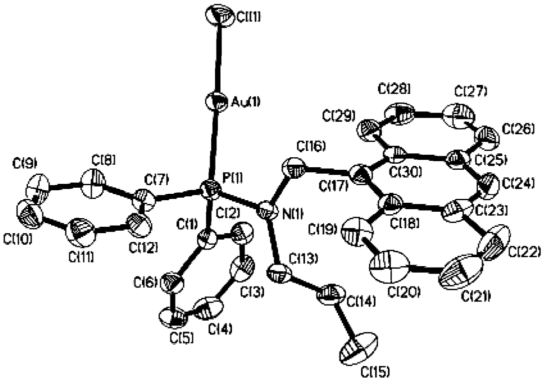

Figure 1. ORTEP drawing for **2** with 30% probability ellipsoids. Selected bond distances (Å) and angles (deg): Au(1)−P(1) 2.234, Au(1)−Cl(1) 2.286; Cl(1)−Au(1)−P(1) 178.37, Au(1)−P(1)−N(1) 112.96.

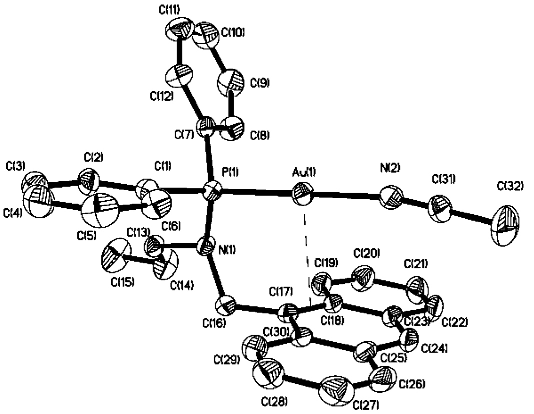

Figure 2. ORTEP drawing for **3a** with 30% probability ellipsoids. Selected bond distances (Å) and angles (deg): Au(1)−C(17) 2.958, Au(1)−C(30) 3.097; P(1)−Au(1)−N(2) 179.59, Au(1)−P(1)−N(1) 111.06, Au(1)−N(2)−C(31) 169.5.

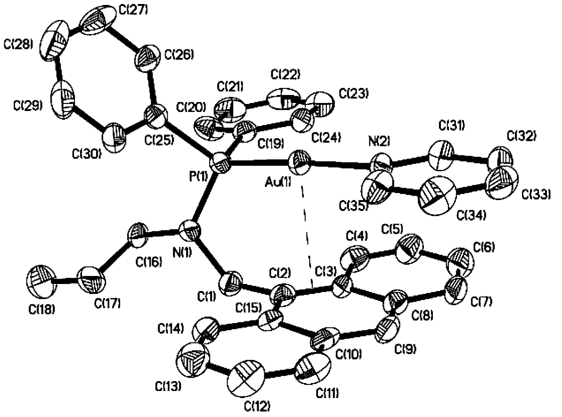

Figure 3. ORTEP drawing for **3b** with 30% probability ellipsoids. Selected bond distances (Å) and angles (deg): Au(1)−C(2) 3.02, Au(1)−C(3) 3.163; P(1)−Au(1)−N(2) 177.07, Au(1)−P(1)−N(1) 112.54.

and 114.4° (**3c**), which are comparable to that of our gold(I) η^6-arene complex (117.43°). In the latter, the existence of the three-center bond has been supported by density functional theory calculation.[3]

The distances of Au(1)−C(17) and Au(1)−C(30) (2.958 and 3.097 Å) in **3a**, Au(1)−C(2) and Au(1)−C(3) (3.020 and 3.163 Å) in **3b**, and Au(1)−C(2) and Au(1)−C(15) (3.077 and 3.119 Å) in **3c** are comparable with those of C arene−Au$^+$ (3.118−3.246 Å) in our gold(I) η^6-arene complex and exhibit a η^2-binding mode between the Au$^+$ and anthracene units. Another feature of complex **3a** is the $\pi-\pi$ interaction between the coordinated acetonitrile and the anthracene unit. The Au(1)−N(2)−C(31) angle (169.5°) has a deviation from linearity and indicates the presence of a secondary interaction with the anthracene unit. The N(2)≡C(31) bond in CH_3CN and the C(24)−C(25) bond in the anthracene ring adopt a cross-configuration, and the distance between the middle points of the two bonds (3.29 Å) is relatively short and comparable with the $\pi-\pi$ stacking distance in graphite. The distances of N(2)−C(24), N(2)−C(25), C(31)−C(24), and C(31)−C(25) fall in the range of 3.349−3.499 Å. The Au(1)−N(2) distance (2.043 Å) is longer than that of the only reported Au$^+$−NCCH$_3$ complex [Au(NCCH$_3$)$_2$][SbF$_6$] (1.97 Å).[6] Whereas there is no the overlapping part between the coordinated pyridine and the anthracene unit in space in **3b** and the dihedral angle is 4.56°, the $\pi-\pi$ interaction does not exist.

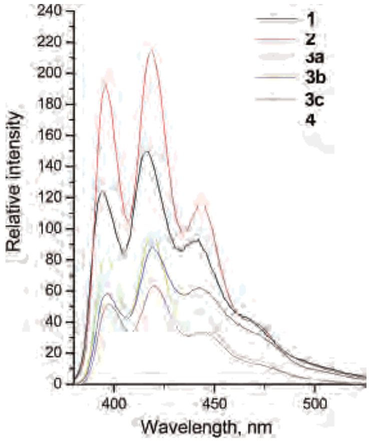

Figure 4. Fluorescence emission spectra ($\lambda_{ex} = 370$ nm) of ligand **1** and complexes **2**, **3a**−**c**, and **4** in CH_2Cl_2.

By treatment with $AgClO_4$ in CH_2Cl_2, **2** can convert to **4**, which has much less fluorescence emission (vide infra) and probably has a stronger η^2−π-coordination action between the Au$^+$ ion and the anthracene unit in comparison with **3a**−**c**. Complex **4** is very sensitive to light and air, cannot be separated out, and has been confirmed by ^{1}H and ^{31}P NMR spectra. **3a**−**c** have unequivocally been proven to be gold(I) η^2-arene complexes.

Now, the question is, why are there different configurations among **2** and **3a**−**c**, all of which include a linear two-coordinated Au$^+$ unit? Compared with the neutral complex **2**, the electron densities on the gold atoms are less than those in complexes **3a**−**c**, which are unfavorable for the donation of a π electron toward the arene units. This point of view conflicts with the widely accepted Dewer−Chatt−Duncanson model,[7] which predicts η^2-bonding of silver(I) to a pair of aromatic carbon atoms by its π back-donation in the silver(1+) arene complexes. According to the Mulliken assumption,[8] the π interaction of arene with gold(I) should be dominated by charge transfer from arene to the Au$^+$ ion.

---

(6) Willner, H.; Schaebs, J.; Hwang, G.; Mistry, F.; Jones, R.; Trotter, J.; Aubke, F. *J. Am. Chem. Soc.* **1992**, *114*, 8972−8980.

(7) (a) Dewar, M. J. S. *Bull. Soc. Chim. Fr.* **1951**, *18*, C79. (b) Chatt, J.; Duncanson, L. A. *J. Chem. Soc.* **1953**, 2939.

(8) Mulliken, R. S. *J. Am. Chem. Soc.* **1952**, *74*, 811.

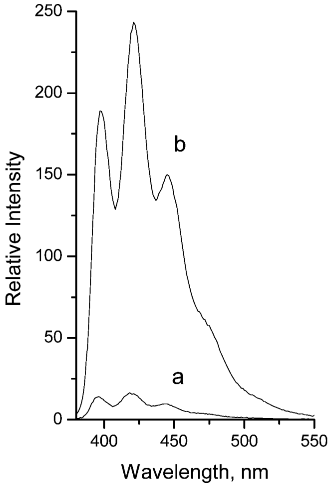

Figure 5. Fluorescence emission spectra ($\lambda_{ex} = 370$ nm) of **4** (was prepared in situ by reacting **2** with $AgClO_4$ in CH_2Cl_2) and **5** (**4** + L_2) in CH_2Cl_2: (a) **4** (1×10^{-5} M) (17); (b) **4** (1×10^{-5} M) + PPh_3 (1 equiv) (243). The digit in parentheses represents the fluorescence relative intensity.

Fluorescence spectra of the free ligand **1** and complexes **2**, **3a**−**c**, and **4** are given in Figure 4. While the free ligand **1** in CH_2Cl_2 exhibits a strong emission centered at 415 nm, complex **2** gives an increased emission, which may be attributed to inhibition of the photoinduced electron transfer effect owing to the P atom donation to the Au atom. The emissions of **3a**−**c** and **4** are weak and feeble owing to the formation of a charge-transfer complex between the anthracene unit and the Au^+ ion. When a solution of **4** or **3a** (1×10^{-5} M) in CH_2Cl_2 is added with an equivalent amount of $L_2(Ph_3P)$, the fluorescence intensity significantly increases (Figure 5 and the Supporting Information). The above-mentioned processes indicate that **5** with the arm-opening configuration can be formed from **3a** or **4** through the ligand substitution or binding reaction. The complex **5** has been confirmed by ^1H, ^{13}C, and ^{31}P NMR spectra and elemental analysis. In the ^{13}C NMR spectrum, the C(9) resonance of the anthracence unit is at 134 ppm in **5**, whereas it is at 133 ppm in **3a**, and the upfield shift indicates that there is a secondary interaction between the anthracene unit and the coordinated acetonitrile owing to the arm-closing configuration.

In summary, **3a**−**c** are the first reported gold(I) η^2-arene complexes. We consider that the formation of these complexes is decided by the following factors: (1) the cationic state of the Au complex is the prerequisite; (2) because of the weak bonding of gold(I) η^2-arene, preserving or breaking the bond to a great extent depends on the steric factor of the incoming ligand in the substitution or binding reaction.

We predict that new gold(I) η^2-arene complexes can be prepared by the reaction of **3a** or **4** with P, N, or S compounds with end-group linear (like $NCCH_3$ and $SPPh_3$) or aromatic planar (like pyridine) structures on the coordinated atoms.

Acknowledgment. We gratefully acknowledge the financial assistance provided by the National Natural Science Foundation of China (Project No. 20472036).

Supporting Information Available: Synthetic procedures for **1**−**5**, crystallographic data for **2** and **3a**−**c** in CIF format, and fluorescence spectra for **3a** and **5**. This material is available free of charge via the Internet at http://pubs.acs.org.

IC051869R